

# The Glashow resonance at IceCube: signatures, event rates and $pp$ vs. $p\gamma$ interactions

Atri Bhattacharya<sup>\*1</sup>, Raj Gandhi<sup>\*2</sup>, Werner Rodejohann<sup>†3</sup>, Atsushi Watanabe<sup>‡,‡4</sup>

<sup>\*</sup>*Harish-Chandra Research Institute, Chhatnag Road, Jhansi, Allahabad 211 019, India*

<sup>†</sup>*Max-Planck-Institut für Kernphysik, Postfach 103980, 69029 Heidelberg, Germany*

<sup>‡</sup>*Department of Physics, Niigata University, Niigata 950-2181, Japan*

(August, 2011)

## Abstract

We revisit the signatures of the Glashow resonance process  $\bar{\nu}_e e \rightarrow W$  in the high-energy astrophysical neutrino observatory IceCube. We note that in addition to the standard hadronic and electromagnetic showers produced by an incoming neutrino at the resonance energy of  $E_\nu \approx 6.3$  PeV, there are two clear signals of the process: the “pure muon” from  $\bar{\nu}_e e \rightarrow \bar{\nu}_\mu \mu$  and the “contained lollipop” from  $\bar{\nu}_e e \rightarrow \bar{\nu}_\tau \tau$ . The event rate and the signal-to-background ratio (the ratio of the resonant to concurrent non-resonant processes) are calculated for each type of interaction, based on current flux limits on the diffuse neutrino flux. Because of the low background in the neighborhood of the resonance, the observation of only one pure muon or contained lollipop event essentially signals discovery of the resonance, even if the expected event numbers are small. We also evaluate the total event rates of the Glashow resonance from the extra-galactic diffuse neutrino flux and emphasize its utility as a discovery tool to enable first observations of such a flux. We find that one can expect 3.6 (0.65) events per year for a pure  $pp$  ( $p\gamma$ ) source, along with an added contribution of 0.51 (0.21) from non-resonant events. We also give results as a function of the ratio of  $pp$  vs  $p\gamma$  sources.

---

<sup>1</sup> atri@hri.res.in

<sup>2</sup> nubarnu@gmail.com

<sup>3</sup> werner.rodejohann@mpi-hd.mpg.de

<sup>4</sup> watanabe@muse.sc.niigata-u.ac.jp

# 1 Introduction

Neutrinos are unique astronomical messengers. The observation of extra-galactic high energy astrophysical neutrinos would imply a hadronic origin of cosmic rays. Moreover, unlike photons or charged particles, they travel across the Universe without deflection by interstellar magnetic fields or absorption by intervening matter. Existing and upcoming neutrino detectors (see for example [1, 2, 3, 4, 5, 6, 7]) are expected to eventually observe high-energy neutrinos from Active Galactic Nuclei, Gamma Ray Bursts, GZK processes and other feasible sources.

High-energy cosmic neutrinos are also unique messengers of physics of and beyond the Standard Model. With a typical baseline of inter-galactic scales, neutrinos propagate incoherently such that the transition probabilities between the flavor eigenstates are described only by the elements of the lepton mixing matrix. The flavor composition at the Earth thus carries important information on the lepton flavor structure [8], see [9] for a recent review. Furthermore, the long baselines and high energies allow for interesting discussions of exotic possibilities such as neutrino decay [10], pseudo-Dirac neutrinos [11], Lorentz and CPT violation [12], which may show an effect in flavor ratio deformations of the diffuse spectrum [13].

Since the ultra-high energy neutrinos span a wide range of energies, they can be sensitive to the Glashow Resonance (GR) [14, 15, 16], which refers to the resonant formation of an intermediate  $W^-$  in  $\bar{\nu}_e e$  collision at the anti-neutrino energy  $E_{\bar{\nu}} = 6.3 \text{ PeV} \simeq 10^{6.8} \text{ GeV}$ . This is a particularly interesting process [17, 18, 19, 20], unique in its sensitivity to only anti-neutrinos. In particular, because the relative  $\bar{\nu}_e$  content of  $pp$  and  $p\gamma$  collision final states is very different, the question of which of these two processes lie at the origin of high energy neutrinos can, in principle, be tested well with GR events. Indeed, earlier works have focused mainly on the resonance detection via shower events and on how the GR can be used as a discriminator of the relative abundance of the  $pp$  and  $p\gamma$  sources.

Our emphasis in this work is not just on the detectability of the resonance itself, but also on its feasibility as a tool to detect the first extra-galactic diffuse neutrino signals. We recalculate expected GR event numbers and their dependence on the relative contribution of  $pp$  and  $p\gamma$  sources. Our work updates and generalizes the results of Ref. [17]. To calculate the number of events, we use the Waxman–Bahcall  $E^{-2}$  spectrum [21] as a benchmark neutrino spectrum. Recently IceCube, the construction of which has been

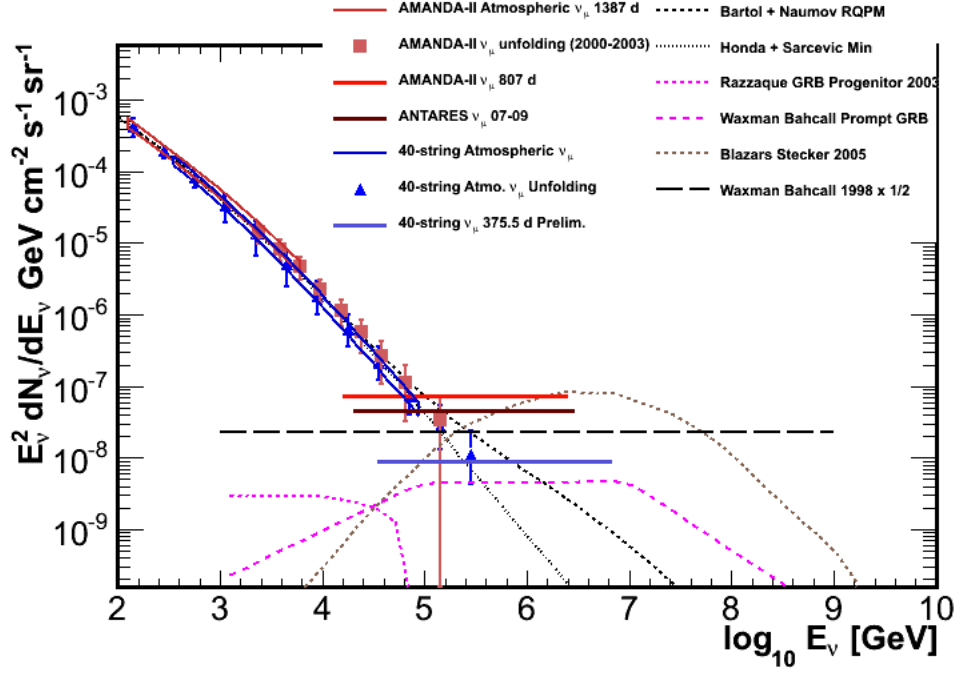


Figure 1: Present experimental bounds from IceCube on the diffuse  $\nu_\mu$  flux assuming an  $E^{-2}$  injection spectrum at source [22]. Predictions of neutrino fluxes from several theoretical models are also shown.

completed in December 2010 with 86 strings, has improved the upper bound of the cosmic neutrino flux [22]. The current limits on the diffuse neutrino flux are shown in Fig. 1. If the neutrino flux is to be observed, it is reasonable to assume that it will emerge above the atmospheric background while staying below the current experimental upper bounds. The present status of these limits leads us to believe that this is likely to happen at energies of  $10^6$  GeV or greater, close to region of the Glashow resonance. Therefore, it is useful and timely to revisit this resonance region carefully to reassess its potential as a tool to detect the cosmic diffuse neutrinos.

In addition, we point out that there are two types of distinctive resonant processes besides the standard shower signatures from  $\bar{\nu}_e e \rightarrow \text{hadrons}$  and  $\bar{\nu}_e e \rightarrow \bar{\nu}_e e$  considered in the literature. We call these new signatures “pure muon” and “contained lollipop” events. A pure muon event occurs when only a muon track (and nothing else) is created inside the detector volume by the resonant process  $\bar{\nu}_e e \rightarrow \bar{\nu}_\mu \mu$ . We sketch the signature in Fig. 2. Unlike the neutrino–nucleon charged current scattering  $\nu_\mu N \rightarrow \mu X$  (and its charge conjugated counterpart), the pure muon track is not accompanied by any shower

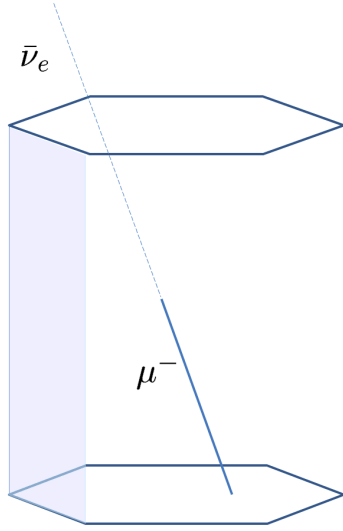


Figure 2: Pure muon

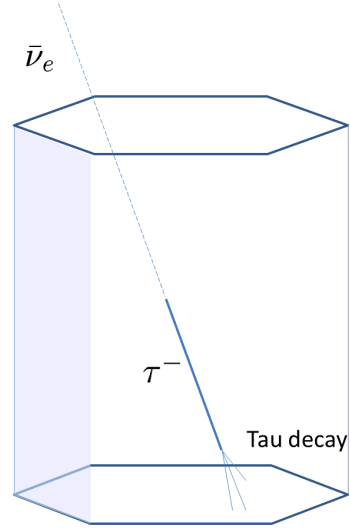


Figure 3: Contained lollipop

activity at its starting point. We note that in  $\nu_\mu N \rightarrow \mu X$  processes with PeV neutrino energies, about 26% of the initial neutrino energy is transferred to the kicked quark, which turns into a hadronic cascade [23]. Thus, a muon track from  $\nu_\mu N \rightarrow \mu X$  is accompanied by a  $\sim 200$  m radius shower at the interaction vertex for PeV neutrino energies. This is clearly distinguishable from the muons of the pure muon event  $\bar{\nu}_e e \rightarrow \bar{\nu}_\mu \mu$ . A possible background against this signal is the non-resonant electroweak process  $\nu_\mu e \rightarrow \mu \nu_e$ . The cross section is however three orders of magnitude smaller than  $\bar{\nu}_e e \rightarrow \bar{\nu}_\mu \mu$  at the resonant energy. The pure muon is therefore essentially background free in the neighborhood of the resonance energy and even one event implies discovery of the resonance and signals the presence of diffuse extra-galactic flux.

A contained lollipop event occurs for  $\bar{\nu}_e e \rightarrow \bar{\nu}_\tau \tau$ : a tau is created and decays inside the detector with a sufficient length of the tau track, see Fig. 3. Again, due to the lack of shower activity at the initial vertex, the contained lollipop is also clearly separated from the standard double bang [24] signature induced by the  $\nu_\tau N + \bar{\nu}_\tau N$  charged current scattering, and it is therefore also essentially free from background.

This paper is organized as follows: in Section 2, we briefly review the cross sections associated with the GR, in Section 3, we discuss the expected neutrino flux for  $pp$  and  $p\gamma$  sources, keeping their relative flux ratio as a free parameter. In Section 4, the event rate

and the signal-to-background ratio are studied, and finally, conclusions are presented in Section 5.

## 2 The Glashow-resonance and its relevance to present day UHE neutrino detection

Ultra-high energy electron anti-neutrinos allow the resonant formation of  $W^-$  in their interactions with electrons, at 6.3 PeV. This process, known as the Glashow resonance [14, 15, 16] has, in the resonance energy band, several notably high cross-sections for the allowed decay channels of the  $W^-$ . In particular, the differential cross-section for  $\bar{\nu}_e e \rightarrow \bar{\nu}_\mu \mu$  is given by

$$\frac{d\sigma}{dy}(\bar{\nu}_e e \rightarrow \bar{\nu}_\mu \mu) = \frac{G_F^2 m E_\nu}{2\pi} \frac{4(1-y)^2 (1 - (\mu^2 - m^2)/2mE_\nu)^2}{(1 - 2mE_\nu/M_W^2)^2 + \Gamma_W^2/M_W^2}, \quad (2.1)$$

and, for hadrons one may write

$$\frac{d\sigma}{dy}(\bar{\nu}_e e \rightarrow \text{hadrons}) = \frac{d\sigma}{dy}(\bar{\nu}_e e \rightarrow \bar{\nu}_\mu \mu) \times \frac{\Gamma(W \rightarrow \text{hadrons})}{\Gamma(W \rightarrow \bar{\nu}_\mu \mu)}. \quad (2.2)$$

The above expressions hold in the lab frame where  $m$  = electron mass,  $\mu$  = muon mass,  $M_W = W^-$  mass,  $y = E_\mu/E_\nu$ , and  $\Gamma_W$  is the total width of the  $W$ .

Table 1 [23] lists the total cross-sections at  $E_\nu^{\text{res}} = 6.3$  PeV. We note that for the leptonic final states, one expects (very nearly) equal cross-sections regardless of whether one produces  $\bar{\nu}_\mu \mu$ ,  $\bar{\nu}_\tau \tau$  or  $\bar{\nu}_e e$ .

In the right panel of Table 1 we list, also at  $E_\nu = 6.3$  PeV, the possible non-resonant interactions which could provide backgrounds to the interactions listed in the left panel of Table 1. We note that the total resonant cross-section,  $\bar{\nu}_e e \rightarrow \text{anything}$  is about 360 times higher than the total neutrino-nucleon cross-section,  $\nu_\mu N \rightarrow \mu + \text{anything}$ . The cross-section for  $\bar{\nu}_e e \rightarrow \text{hadrons}$  is about 240 times its non-resonant hadron producing background interaction  $\nu_\mu N \rightarrow \mu + \text{anything}$ . Even the resonant leptonic final state interactions have cross-sections about 40 times that of the total  $\nu_\mu N \rightarrow \mu + \text{anything}$  cross-section. Finally we note that the “pure-muon” and “contained lollipop” resonant processes discussed in the Sec. 1 have negligible backgrounds. For example, the process  $\bar{\nu}_e e \rightarrow \bar{\nu}_\mu \mu$  (pure muon) has a cross-section about 1000 times higher than its non-resonant counterpart  $\nu_\mu e \rightarrow \nu_e \mu$ .

Interaction	$\sigma$ [cm <sup>2</sup> ]	Interaction	$\sigma$ [cm <sup>2</sup> ]
$\bar{\nu}_e e \rightarrow \bar{\nu}_e e$	$5.38 \times 10^{-32}$	$\nu_\mu N \rightarrow \mu + \text{anything}$	$1.43 \times 10^{-33}$
$\bar{\nu}_e e \rightarrow \bar{\nu}_\mu \mu$	$5.38 \times 10^{-32}$	$\nu_\mu N \rightarrow \nu_\mu + \text{anything}$	$6.04 \times 10^{-34}$
$\bar{\nu}_e e \rightarrow \bar{\nu}_\tau \tau$	$5.38 \times 10^{-32}$	$\nu_\mu e \rightarrow \nu_e \mu$	$5.42 \times 10^{-35}$
$\bar{\nu}_e e \rightarrow \text{hadrons}$	$3.41 \times 10^{-31}$		
$\bar{\nu}_e e \rightarrow \text{anything}$	$5.02 \times 10^{-31}$		

Table 1: Resonant GR cross-sections for electron anti-neutrino (left panel) and non-resonant (right panel) interactions at  $E = 6.3$  PeV.

Given these considerations and the fact that the present bounds shown in Fig. 1 restrict observational diffuse fluxes to energies above  $10^6$  GeV (*i.e.*, close to the GR region), the GR, in spite of its narrow span of energy, may be an important discovery tool for the yet to be observed extra-galactic diffuse neutrino spectrum.

### 3 Diffuse Neutrino Fluxes for $pp$ and $p\gamma$ sources

The search for cosmic neutrinos with PeV energies is motivated by observations of cosmic rays. It has been conjectured that cosmic ray engines accelerate protons and confine them with magnetic fields in the acceleration region. The accelerated protons interact with ambient photons or protons, producing neutrons and charged pions. Charged particles are trapped by magnetic fields, while neutral particles escape from the source region, decay and produce observable cosmic rays and neutrinos. If the source region is optically thin, the energy density of neutrinos scales linearly with the cosmic ray density and the neutrino intensities are co-related with the observed cosmic ray flux.

The result of these considerations for the expected total neutrino flux (the sum over all species) at the source is the Waxman-Bahcall flux, given by [21]

$$E_\nu^2 \Phi_{\nu+\bar{\nu}} = 2 \times 10^{-8} \epsilon_\pi \xi_z \quad (\text{GeV cm}^{-2} \text{s}^{-1} \text{sr}^{-1}). \quad (3.1)$$

Here  $\xi_z$  is a function of the red-shift parameter  $z$  alone, representing the evolution of sources with red-shift, and  $\epsilon_\pi$  is the ratio of pion energy to the emerging nucleon energy at the source. One has  $\xi_z \approx 0.6$  for no source evolution, while  $\xi_z \approx 3$  for an evolution  $\propto (1+z)^3$ . Depending on the relative ambient gas and photon densities, the neutrino production originates in either  $p\gamma$  or  $pp$  interactions. For the  $pp$  case  $\epsilon_\pi \approx 0.6$  and for the  $p\gamma$  case  $\epsilon_\pi \approx 0.25$ .

Since source distributions and types are not well known, we parameterize the relative  $pp$  and  $p\gamma$  contributions to the total flux with a dimensionless parameter  $x$ ,  $0 \leq x \leq 1$ , so that

$$\Phi_{\text{source}} = x\Phi_{\text{source}}^{pp} + (1-x)\Phi_{\text{source}}^{p\gamma}, \quad (3.2)$$

where  $\Phi^{pp/p\gamma}$  represents the neutrino flux from  $pp/p\gamma$  interactions. We assume here that neutron decays, which (as discussed in [19]) could be present in certain sources give negligible contributions to the overall flux. Effects like multi-pion processes producing  $\pi^-$  events in  $p\gamma$  sources, can be included in the parameterization.

The flavor composition at the source is given by  $(\nu_e, \nu_\mu, \nu_\tau) = (\bar{\nu}_e, \bar{\nu}_\mu, \bar{\nu}_\tau) \approx (1, 2, 0)$  for a  $pp$  source and  $(\nu_e, \nu_\mu, \nu_\tau) \approx (1, 1, 0)$  and  $(\bar{\nu}_e, \bar{\nu}_\mu, \bar{\nu}_\tau) \approx (0, 1, 0)$  for the  $p\gamma$  case. These configurations are changed by the incoherent propagation from the source to earth. The transition probabilities between flavor eigenstates are described by three mixing angles and one CP violating phase. By using  $\theta_{12} = 35^\circ$ ,  $\theta_{13} = 0$ , and  $\theta_{23} = 45^\circ$  as reference values of the lepton mixing angles, the flavor ratios at the earth become  $(\nu_e, \nu_\mu, \nu_\tau) = (\bar{\nu}_e, \bar{\nu}_\mu, \bar{\nu}_\tau) = (1, 1, 1)$  for  $pp$ , while  $(\nu_e, \nu_\mu, \nu_\tau) = (0.78, 0.61, 0.61)$  and  $(\bar{\nu}_e, \bar{\nu}_\mu, \bar{\nu}_\tau) = (0.22, 0.39, 0.39)$  for fluxes from  $p\gamma$  interactions. Finally, the flux for each neutrino species is given by

$$E_\nu^2 \Phi_{\nu_e} = 2 \times 10^{-8} \xi_z \left[ x \frac{1}{6} \cdot 0.6 + (1-x) \frac{0.78}{3} \cdot 0.25 \right], \quad (3.3)$$

$$E_\nu^2 \Phi_{\nu_\mu} = 2 \times 10^{-8} \xi_z \left[ x \frac{1}{6} \cdot 0.6 + (1-x) \frac{0.61}{3} \cdot 0.25 \right] = E_\nu^2 \Phi_{\nu_\tau}, \quad (3.4)$$

$$E_\nu^2 \Phi_{\bar{\nu}_e} = 2 \times 10^{-8} \xi_z \left[ x \frac{1}{6} \cdot 0.6 + (1-x) \frac{0.22}{3} \cdot 0.25 \right], \quad (3.5)$$

$$E_\nu^2 \Phi_{\bar{\nu}_\mu} = 2 \times 10^{-8} \xi_z \left[ x \frac{1}{6} \cdot 0.6 + (1-x) \frac{0.39}{3} \cdot 0.25 \right] = E_\nu^2 \Phi_{\bar{\nu}_\tau}, \quad (3.6)$$

in units of  $\text{GeV cm}^{-2} \text{s}^{-1} \text{sr}^{-1}$ . The equalities between  $\nu_\mu$  and  $\nu_\tau$  flavors, both for neutrinos and anti-neutrinos, are the consequence of vanishing  $\theta_{13}$  (actually, vanishing of the real part of  $U_{e3}$  would suffice) and maximal  $\theta_{23}$  used in the calculation. The uncertainty in  $\theta_{13}$  and  $\theta_{23}$  breaks this equality and changes each flux by at most 10%. Note that the total intensity becomes maximal for the pure  $pp$  case  $x = 1$ . With a strong evolution value  $\xi_z = 3$ , the maximal value is  $\sum_\alpha E_\nu^2 \Phi_{\nu_\alpha + \bar{\nu}_\alpha} = 3.6 \times 10^{-8} \text{GeV cm}^{-2} \text{s}^{-1} \text{sr}^{-1}$ , which agrees with the latest upper bound on the  $E^{-2}$  spectrum [22]. In what follows, we use these fluxes with  $\xi_z = 3$  as an example to calculate the event rates.

## 4 Event rates and signal/background ratio

As discussed before, we will look at both shower and muon/tau-track events to identify unique signatures for cosmic neutrinos via the Glashow resonance. In this context, we first focus on the shower events.

### 4.1 Shower signatures of the Glashow resonance

Among the resonance processes, it turns out that the only channel significantly contributing to the events is the hadronic interaction  $\bar{\nu}_e e \rightarrow \text{hadrons}$ , while the contributions from the other channels are negligibly small. Beside the hadronic channel, the following two decay modes produce electromagnetic showers in the detector; *i*)  $\bar{\nu}_e e \rightarrow \bar{\nu}_e e$  and *ii*)  $\bar{\nu}_e e \rightarrow \bar{\nu}_\tau \tau$  with  $E_\tau \lesssim 2 \text{ PeV}$ . A tau of  $E_\tau \gtrsim 2 \text{ PeV}$  travels more than 100 m before decay and can be separated from a single shower<sup>¶</sup>. Notice that the hadronic channel constitutes 68% of the total decay width of  $W^-$ , whereas *i*) and *ii*) constitute 11% each. Furthermore, only half of the parent neutrino energy becomes shower energy in *i*) and *ii*), while all energy is converted to shower energy in the hadronic mode.

The event rate of  $\bar{\nu}_e e \rightarrow \text{hadrons}$  is calculated as

$$\text{Rate} = 2\pi \frac{10}{18} N_A V_{\text{eff}} \int dE_\nu \int_0^1 dy \frac{d\sigma}{dy} \Phi_{\bar{\nu}_e}(E_\nu), \quad (4.1)$$

where  $N_A = 6.022 \times 10^{23} \text{ cm}^{-3}$  and  $V_{\text{eff}} \approx 2 \text{ km}^3$ , and  $d\sigma/dy$  is the neutrino–electron cross section [23]. The effective volume is taken as twice as large as the instrumental volume since the radius of the showers with the resonant energy is about 300 m. The events are integrated over the upper half sphere since up-moving electron neutrinos are attenuated by the earth matter. At the resonance peak, the integrated cross section is  $3.4 \times 10^{-31} \text{ cm}^2$ . With the  $pp$  ( $p\gamma$ ) source flux  $E_\nu^2 \Phi_{\bar{\nu}_e} = 6 (1.1) \times 10^{-9} \text{ GeV cm}^{-2} \text{ s}^{-1} \text{ sr}^{-1}$ , 3.2 (0.6) events are expected at the resonant energy region for 1 year of observation. The off-resonant background events receive contributions from  $\nu_e N + \bar{\nu}_e N$  (CC) and  $\nu_\alpha N + \bar{\nu}_\alpha N$  (NC), where CC (NC) represents the charged (neutral) current. The tau contribution  $\nu_\tau N + \bar{\nu}_\tau N$  (CC) is irrelevant at the resonance energy bin since a tau with  $E_\tau \gtrsim 2 \text{ PeV}$  manifests itself as a track. The event rate of  $\nu_e N + \bar{\nu}_e N$  (CC) is given by

$$\text{Rate} = 2\pi N_A V_{\text{eff}} \int dE_\nu [\sigma_{\text{CC}}(\nu N) \Phi_{\nu_e}(E_\nu) + \sigma_{\text{CC}}(\bar{\nu} N) \Phi_{\bar{\nu}_e}(E_\nu)], \quad (4.2)$$

---

<sup>¶</sup>This is identified as the contained lollipop if the shower provided by the tau decay occurs inside the detector volume.



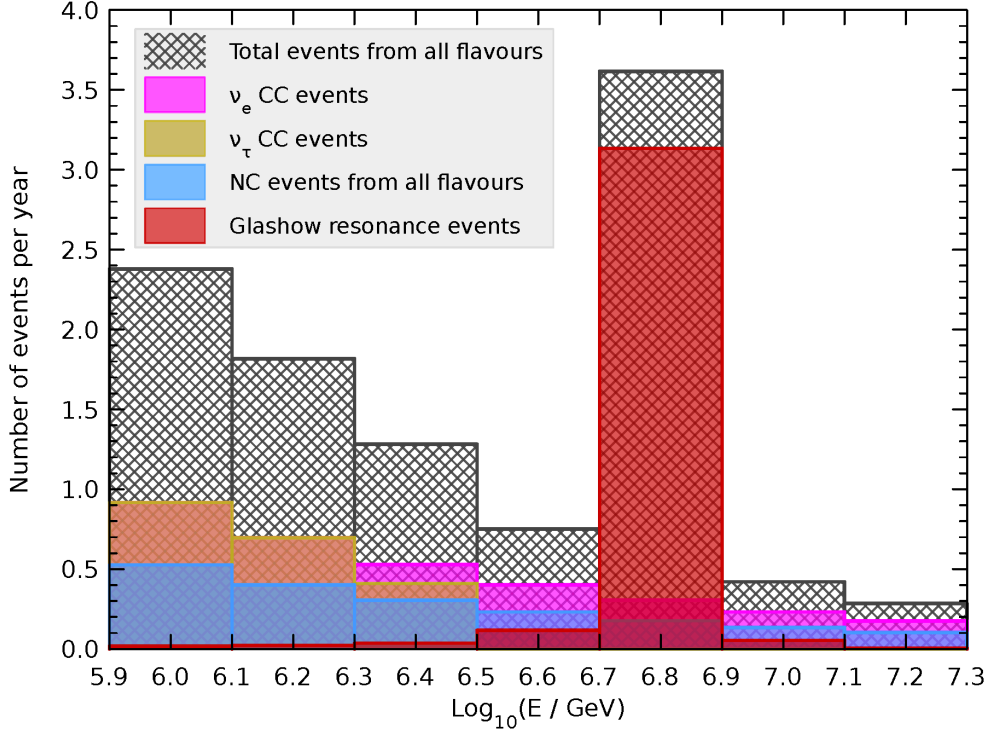


Figure 4: The shower spectrum for pure  $pp$  sources,  $x = 1$ . We have neglected events from the interactions  $\bar{\nu}_e e \rightarrow \bar{\nu}_e e$  and  $\bar{\nu}_e e \rightarrow \bar{\nu}_\tau \tau$  which contribute, comparatively, a very tiny fraction of events to the spectrum.

where  $\sigma_{CC}(\nu N/\bar{\nu} N)$  is the neutrino–nucleon cross section which is  $\approx 1.4 \times 10^{-33} \text{ cm}^2$  at  $E_\nu = 6.3 \text{ PeV}$  [23]. For  $\nu_\alpha N + \bar{\nu}_\alpha N$  (NC), the rate is calculated as

$$\text{Rate} \simeq 2\pi N_A V_{\text{eff}} \sum_{\alpha=e,\mu,\tau} \int_{E_0/\langle y \rangle}^{E_1/\langle y \rangle} dE_\nu [\sigma_{\text{NC}}(\nu N) \Phi_{\nu_\alpha}(E_\nu) + \sigma_{\text{NC}}(\bar{\nu} N) \Phi_{\bar{\nu}_\alpha}(E_\nu)], \quad (4.3)$$

for the shower energy between  $E_0$  and  $E_1$ . Here  $\langle y \rangle$  is the mean inelasticity which is well described by the average value  $\langle y \rangle = 0.26$  at PeV energies. The NC cross section at the resonant peak is  $\approx 6 \times 10^{-34} \text{ cm}^2$ . In the NC process, only a part of the neutrino energy (about 26%) is converted to shower energy, so that the NC contribution is generally small with respect to the CC event number. We have assumed 100% shadowing by the earth for the sake of simplicity, but note that muon and tau neutrinos are not completely attenuated and actually about 20% of them survive in average at the resonant energy. The muon and tau component in Eq. (4.3) would thus receive  $\simeq 20\%$  enhancement in a more precise treatment. For showers with energies  $10^{6.7} \text{ GeV} < E_{\text{shower}} < 10^{6.9} \text{ GeV}$ , for

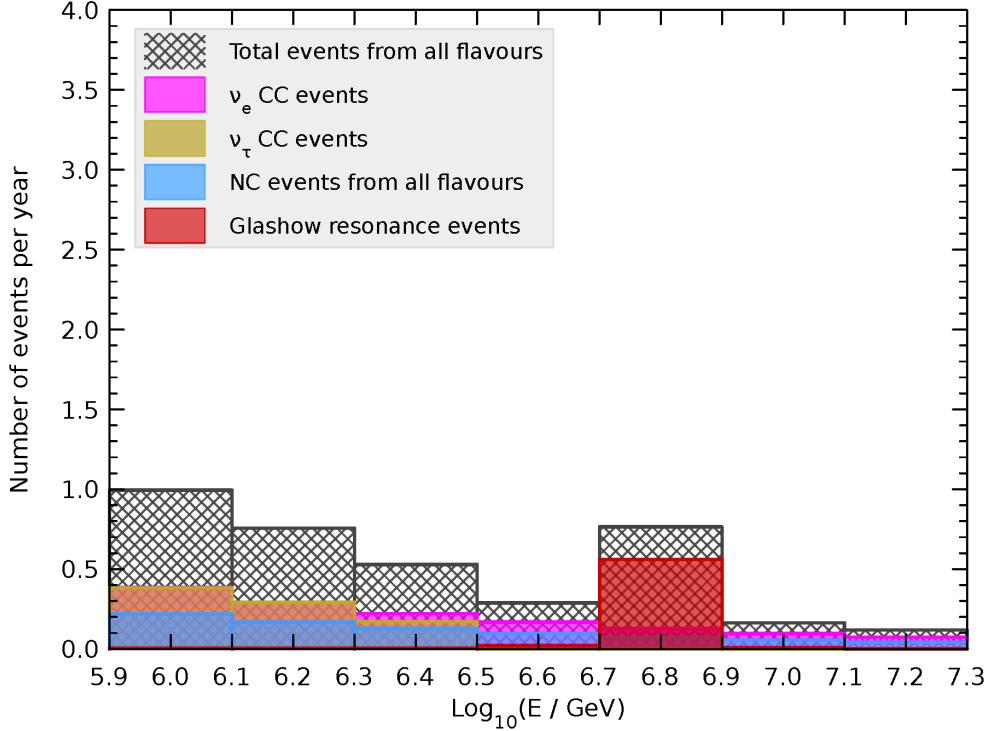


Figure 5: The shower spectrum for pure  $p\gamma$  sources,  $x = 0$ . We have neglected events from the interactions  $\bar{\nu}_e e \rightarrow \bar{\nu}_e e$  and  $\bar{\nu}_e e \rightarrow \bar{\nu}_e \tau$  which contribute, comparatively, a very tiny fraction of events to the spectrum.

example, the rate reads  $0.31 \text{ yr}^{-1}$  for CC and  $0.18 \text{ yr}^{-1}$  for NC in the case of a  $pp$  flux.

Figs. 4 and 5 show the number of events in the neighborhood of the resonant energy. Fig. 4 is for a pure  $pp$  flux with  $x = 1$  and Fig. 5 for a pure  $p\gamma$  flux  $x = 0$ . As was pointed out in [17], the resonance peak is clearly seen for a pure  $pp$  source, whereas the peak is significantly weakened for  $p\gamma$  sources. We have divided the energy decade  $10^{6.3} \text{ GeV} < E_{\text{shower}} < 10^{7.3} \text{ GeV}$  into five bins by assuming the energy resolution of the shower to be  $\log_{10}(E_{\text{shower}}/\text{GeV}) = 0.2$ . Notice that  $\nu_\tau N + \bar{\nu}_\tau N$  and  $\nu_e N + \bar{\nu}_e N$  generate the same event numbers at low energies in Fig. 4, since the cross section and the  $pp$  fluxes are flavor blind. For energies higher than  $10^{6.5} \text{ GeV}$ , events numbers from  $\nu_\tau N + \bar{\nu}_\tau N$  are lower because the tau track becomes visible and the events can be separated from a single shower. Fig. 6 shows the ratio of  $\bar{\nu}_e e \rightarrow \text{hadrons}$  to the sum of all off-resonant processes in the resonant bin  $10^{6.7} \text{ GeV} < E_{\text{shower}} < 10^{6.9} \text{ GeV}$  as a function of  $x$ . The ratio rises from 3 at  $x = 0$  to about 7 at  $x = 1$ .

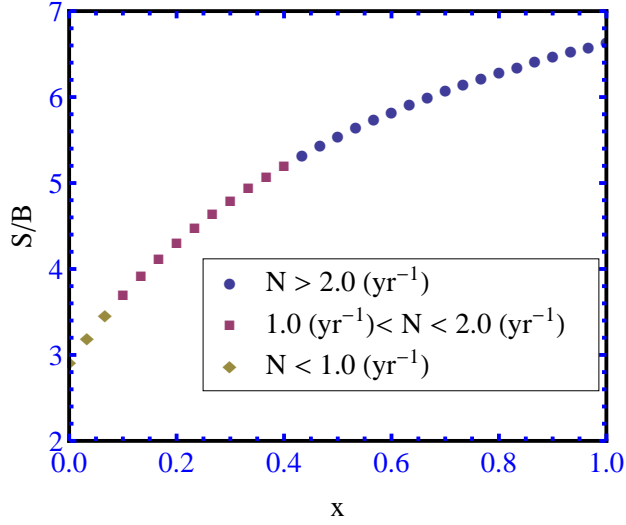


Figure 6: The ratio of  $\bar{\nu}_e e \rightarrow \text{hadrons}$  to the off-resonant processes in the resonant bin as a function of  $x$ .  $N$  represents the total number of event in the resonant bin.

While the total spectral shape shown in Fig. 4 and 5 crucially depends on the parameter  $x$ , it also depends on the flavor composition at the earth. For example, if the muon and tau components would evanesce while the (anti-)electron would stay constant, perhaps due to non-standard physical effects affecting the oscillation probabilities, the ratio of the resonant to off-resonant events is enhanced over the “standard” maximal value set by  $x = 1$ . In an opposite case where only the electron component is damped, the ratio would be anomalously small. Hence the shower spectral shape around the resonance has certain sensitivities to the deformation of the flavor composition, being a complementary test to the shower/muon track ratio. This issue is separately studied in [25].

## 4.2 Novel signatures of the Glashow resonance

We now discuss other unique signatures of the Glashow resonance; the pure muon and the contained lollipop. If the resonant process  $\bar{\nu}_e e \rightarrow \bar{\nu}_\mu \mu$  takes place in the detector volume, it will be observed as a muon track without shower activities at its starting point, see Fig. 2. This “pure muon” signature will be clearly distinguishable from the usual muon track from  $\nu_\mu N$  charged current interactions. The probability that the shower associated with the  $\nu_\mu N$  CC process does not reach the detection threshold is extremely small at PeV energies. There is a possibility that bremsstrahlung of the pure muon may distort

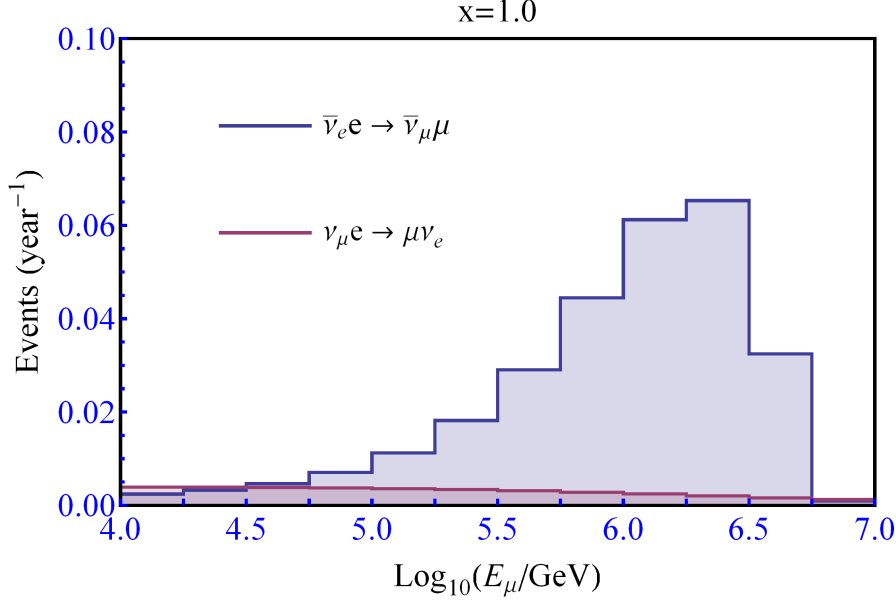


Figure 7: The number of pure  $\mu$  events as the functions of the muon energy for a pure  $pp$  source,  $x = 1$ .

the signal. However, this bremsstrahlung occurs only about 10% of the time, and the energy fraction carried by the radiation is much smaller than  $\langle y \rangle = 0.26$  of the shower. Therefore the probability that the signal is misidentified as the  $\nu_\mu N \rightarrow \mu X$  is expected to be small. The only remaining candidate for background is thus the muon created by the non-resonant process  $\nu_\mu e \rightarrow \mu \nu_e$ .

The event rate of  $\bar{\nu}_e e \rightarrow \bar{\nu}_\mu \mu$  with the muon energy  $E_0 < E_\mu < E_1$  is calculated by

$$\text{Rate} = 2\pi \frac{10}{18} N_A V \left[ \int_{E_0}^{E_1} dE_\nu \int_{\frac{E_0}{E_\nu}}^1 dy + \int_{E_1}^{\infty} dE_\nu \int_{\frac{E_0}{E_\nu}}^{\frac{E_1}{E_\nu}} dy \right] \frac{d\sigma(\bar{\nu}_e e \rightarrow \bar{\nu}_\mu \mu)}{dy} \Phi_{\bar{\nu}_e}(E_\nu), \quad (4.4)$$

where  $V = 1 \text{ km}^3$  is the instrumental volume of IceCube. The non-resonant process  $\nu_\mu e \rightarrow \mu \nu_e$  is also calculated in the same manner by replacing the cross section and the flux.

Fig. 7 shows the event number spectrum of these processes. It is seen that  $\bar{\nu}_e e \rightarrow \bar{\nu}_\mu \mu$  is dominant in the energy regime  $5.0 < \log_{10}(E_\mu/\text{GeV}) < 6.75$ , where the  $\nu_\mu e \rightarrow \mu \nu_e$  contribution is tiny for  $x = 1$ . The integrated number of resonant events in this region is  $0.26 \text{ yr}^{-1}$ . Although the absolute number of the expected event is small, even a single detection of the pure muon event becomes essentially a discovery of the resonance at this energy regime due to its uniqueness. For  $x = 0$ , the rate decreases to  $0.048 \text{ yr}^{-1}$ .

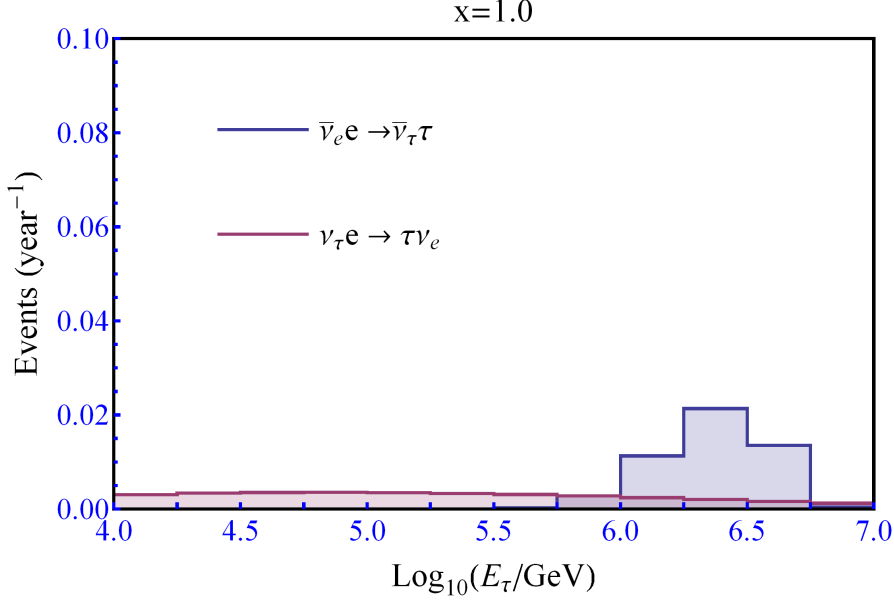


Figure 8: The event spectrum of the contained lollipop for a pure  $pp$  source,  $x = 1$ .

Turning to the contained lollipop, this signature denotes the case when the resonant process  $\bar{\nu}_e e \rightarrow \bar{\nu}_\tau \tau$  takes place in the detector volume and the tau decays a significant distance thereafter, see Fig. 3. This will be observed as a tau track popping up inside the detector (without an initial hadronic shower) and a subsequent shower when it decays at the end of the track. It is a “double-bang without the first bang” so to speak. The event rate with the tau energy of  $E_0 < E_\tau < E_1$  is given by

$$\begin{aligned} \text{Rate} = 2\pi \frac{10}{18} N_A A \left[ \int_{E_0}^{E_1} dE_\nu \int_{\frac{E_0}{E_\nu}}^1 dy + \int_{E_1}^{\infty} dE_\nu \int_{\frac{E_0}{E_\nu}}^{\frac{E_1}{E_\nu}} dy \right] \frac{d\sigma(\bar{\nu}_e e \rightarrow \bar{\nu}_\tau \tau)}{dy} \Phi_{\bar{\nu}_e}(E_\nu) \\ \times \int_{L_0}^{L_1 - x_{\min}} dx_0 \int_{x_0 + x_{\min}}^{L_1} dx \frac{1}{R_\tau} e^{-\frac{x - x_0}{R_\tau}}, \end{aligned} \quad (4.5)$$

where  $R_\tau$  is the tau range  $R_\tau \simeq c\tau y E_\nu / m_\tau$ , and  $A \approx 1 \text{ km}^2$  is the effective area of the detector,  $L_1 - L_0 = L = 1 \text{ km}$  is the length of the detector,  $x_0$  is the neutrino interaction point, and  $x_{\min}$  is the minimum length to separate the tau decay point from the tau creation point. We take  $x_{\min} = 100 \text{ m}$  as a reference value. The exponential factor accounts for the probability with which a tau created at the point  $x_0$  decays at the point  $x$ .

Fig. 8 shows the event spectrum for  $x = 1$  in comparison with the obvious candidate of the background,  $\nu_\tau e \rightarrow \tau \nu_e$ . The contained lollipop dominates in the  $6.0 <$

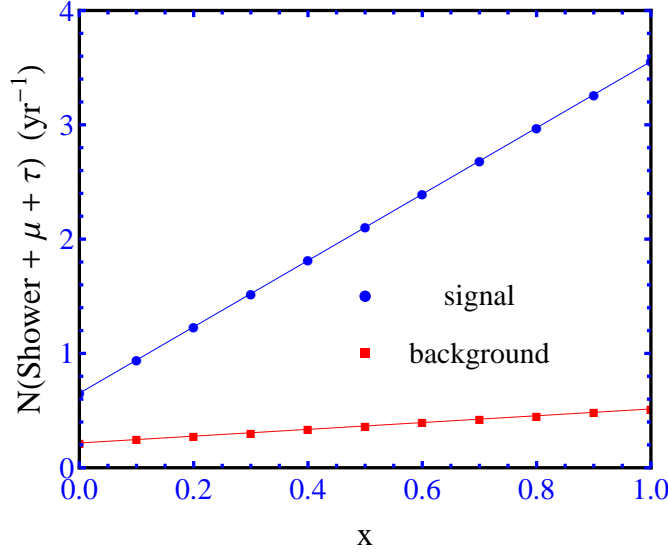


Figure 9: Total number of the Glashow resonance signal as a function of  $x$ . The lower (red) curve shows the background (*i.e.*, off-resonant processes).

$\log_{10}(E_\tau/\text{GeV}) < 6.75$  regime. The integrated number of events in this region is  $0.046 \text{ yr}^{-1}$ . As the pure muon case, observation of a single event would essentially become discovery of the resonance. Note however that the expected event number is about five times smaller than the one from the pure muon signature.

Finally let us define the total signal of the Glashow resonance as the sum of shower, muon track and contained lollipop events. That is,

$$N(\text{Shower} + \mu + \tau) \equiv N(\bar{\nu}_e e \rightarrow \text{hadrons}) + N(\bar{\nu}_e e \rightarrow \bar{\nu}_\mu \mu) + N(\bar{\nu}_e e \rightarrow \bar{\nu}_\tau \tau), \quad (4.6)$$

where  $N(\bar{\nu}_e e \rightarrow \text{hadrons})$  is the number of shower events in  $6.7 < \log_{10}(E_{\text{shower}}) < 6.9$  induced by  $\bar{\nu}_e e \rightarrow \text{hadrons}$ ,  $N(\bar{\nu}_e e \rightarrow \bar{\nu}_\mu \mu)$  is the number of pure muon events in  $5.0 < \log_{10}(E_\mu/\text{GeV}) < 6.75$ , and  $N(\bar{\nu}_e e \rightarrow \bar{\nu}_\tau \tau)$  is the number of contained lollipop events in  $6.0 < \log_{10}(E_\tau/\text{GeV}) < 6.75$ . Fig. 9 presents the total number of the GR events as a function of  $x$ . The background (*i.e.*, the off-resonant contributions) is defined by the summation of the total shower events other than  $\bar{\nu}_e e \rightarrow \text{hadrons}$  in  $6.7 < \log_{10}(E_{\text{shower}}) < 6.9$ , the number of events for  $\nu_\mu e \rightarrow \mu \nu_e$  in  $5.0 < \log_{10}(E_\mu/\text{GeV}) < 6.75$  and for  $\nu_\tau e \rightarrow \tau \nu_e$  in  $6.0 < \log_{10}(E_\tau/\text{GeV}) < 6.75$ . The signal/background ratio rises from  $\simeq 3$  at  $x = 0$  to  $\simeq 7$  at  $x = 1$ . For  $x = 1$ , 7.2 signal events against about 1 background event are expected with 2 years of data accumulation, which is well above the 99% C.L. upper

$x$	Non-resonance	GR	Total
0.0	0.21	0.65	0.86
0.5	0.37	2.1	2.5
1.0	0.51	3.6	4.1

Table 2: A list of expected numbers of events for 1 year data taking in IceCube.

limit for the background only (observation of 1 expected background event corresponds to an upper limit of 5.79 events at 99% C.L. [26]). For  $x = 0.5$ , 6.3 signal events and about 1 background event is expected with 3 years of data accumulation. For the pure  $p\gamma$  case  $x = 0$ , 6.5 signal and about 2 background events are expected within 10 years of data accumulation, which is slightly below the 99% C.L. upper limit for background only observation (observation of 2 expected background events corresponds to an upper limit of 6.69 events at 99% C.L. [26]). Table 2 shows the non-resonant, Glashow resonance and total number of events for three representative values of  $x$ . Depending on the relative abundance of the  $pp$  and  $p\gamma$  sources, 20, 12 and 4 events are expected in IceCube in 5 years.

Our focus in this section was on signatures and event numbers of the Glashow resonance. From the more general point of view of discovery of high-energy cosmic neutrinos however, the off-resonant events (treated as backgrounds so far) are also signals, being distinctive of neutrinos at energies which could not possibly be produced at any other neutrino source. Atmospheric neutrinos are not a significant background for such a discovery since their fluxes are negligibly low at PeV energies and their contribution, consequently, is insignificant.

## 5 Conclusion

We have studied the Glashow resonance in the high-energy astrophysical neutrino observatory IceCube. Besides the standard hadronic/electromagnetic cascade, the pure muon from  $\bar{\nu}_e e \rightarrow \bar{\nu}_\mu \mu$  and the contained lollipop signatures from  $\bar{\nu}_e e \rightarrow \bar{\nu}_\tau \tau$  were identified as clear signals of the resonance. Applying a Waxman-Bahcall  $E^{-2}$  flux in agreement with recent limits, the event numbers for general  $pp$  and  $p\gamma$  sources were evaluated. If the neutrino fluxes are positioned with such intensities as presently conjectured, the confirmation of the resonance is possible with several years of data collection at IceCube.

The resonance could be used as a discovery tool for diffuse astrophysical neutrinos at PeV energies, and to obtain important information about cosmic-rays and astrophysical sources.

## Acknowledgments

We thank Walter Winter for helpful discussions. A.B. would like to thank the Particle and Astroparticle Division of the Max-Planck-Institut für Kernphysik at Heidelberg for hospitality while the work was in progress. R.G. would like to thank the University of Wisconsin phenomenology group and the CERN Theory Division for hospitality while this work was in progress. He would also like to acknowledge financial support from the DAE XI Plan Neutrino project. W.R. is supported by the ERC under the Starting Grant MANITOP and by the DFG in the project RO 2516/4-1 as well as in the Transregio 27. The work of A.W. is supported by the Young Researcher Overseas Visits Program for Vitalizing Brain Circulation Japanese in JSPS.

## References

- [1] B. Baret [IceCube Collaboration], J. Phys. Conf. Ser. **110** (2008) 062001.
- [2] F. Halzen, J. Phys. Conf. Ser. **171** (2009) 012014.
- [3] V. Aynutdinov, A. Avrorin, V. Balkanov, I. Belolaptikov, D. Bogorodsky, N. Budnev, I. Danilchenko, G. Domogatsky *et al.*, Nucl. Instrum. Meth. **A602** (2009) 14-20.
- [4] A. Margiotta [ANTARES Collaboration], Nucl. Phys. Proc. Suppl. **190** (2009) 121-126; J. A. Aguilar *et al.* [ANTARES Collaboration], Phys. Lett. **B696** (2011) 16-22.
- [5] D. Z. Besson, J. Phys. Conf. Ser. **81** (2007) 012008; I. Kravchenko, D. Seckel, D. Besson, J. Ralston, J. Taylor, K. Ratzlaff, R. Young, arXiv:1106.1164.
- [6] P. W. Gorham, P. Allison, S. W. Barwick, J. J. Beatty, D. Z. Besson, W. R. Binns, C. Chen, P. Chen *et al.*, J. Phys. Conf. Ser. **136** (2008) 022052; P. W. Gorham *et al.* [The ANITA Collaboration], Phys. Rev. **D82** (2010) 022004.
- [7] A. Margiotta [KM3NeT Collaboration], J. Phys. Conf. Ser. **203** (2010) 012124.



- [8] See e.g., H. Athar, M. Jezabek, O. Yasuda, Phys. Rev. **D62** (2000) 103007; G. Barenboim, C. Quigg, Phys. Rev. **D67** (2003) 073024; J. F. Beacom, N. F. Bell, D. Hooper, S. Pakvasa, T. J. Weiler, Phys. Rev. **D68** (2003) 093005; P. D. Serpico, M. Kachelriess, Phys. Rev. Lett. **94** (2005) 211102; Z. -z. Xing, Phys. Rev. **D74** (2006) 013009; W. Rodejohann, JCAP **0701** (2007) 029; P. Lipari, M. Lusignoli, D. Meloni, Phys. Rev. **D75** (2007) 123005; K. Blum, Y. Nir, E. Waxman, arXiv:0706.2070; S. Pakvasa, W. Rodejohann, T. J. Weiler, JHEP **0802** (2008) 005; A. Esmaili, Y. Farzan, Nucl. Phys. **B821** (2009) 197-214; S. Choubey, W. Rodejohann, Phys. Rev. **D80**, 113006 (2009).
- [9] S. Pakvasa, Mod. Phys. Lett. **A23** (2008) 1313-1324.
- [10] J. F. Beacom, N. F. Bell, D. Hooper, S. Pakvasa, T. J. Weiler, Phys. Rev. Lett. **90** (2003) 181301; Phys. Rev. **D69** (2004) 017303; M. Maltoni, W. Winter, JHEP **0807** (2008) 064.
- [11] J. F. Beacom, N. F. Bell, D. Hooper, J. G. Learned, S. Pakvasa, T. J. Weiler, Phys. Rev. Lett. **92** (2004) 011101; P. Keranen, J. Maalampi, M. Myyrylainen, J. Riittinen, Phys. Lett. **B574** (2003) 162-168; A. Esmaili, Phys. Rev. **D81** (2010) 013006; J. Barry, R. N. Mohapatra, W. Rodejohann, Phys. Rev. **D83** (2011) 113012.
- [12] D. Hooper, D. Morgan, E. Winstanley, Phys. Rev. **D72** (2005) 065009.
- [13] A. Bhattacharya, S. Choubey, R. Gandhi, A. Watanabe, Phys. Lett. **B690** (2010) 42-47; JCAP **1009** (2010) 009.
- [14] S. L. Glashow, Phys. Rev. **118** (1960) 316-317.
- [15] V. S. Berezinsky, A. Z. Gazizov, JETP Lett. **25** (1977) 254-256.
- [16] V. S. Berezinsky, A. Z. Gazizov, Sov. J. Nucl. Phys. **33** (1981) 120-125.
- [17] L. A. Anchordoqui, H. Goldberg, F. Halzen, T. J. Weiler, Phys. Lett. **B621** (2005) 18-21.
- [18] P. Bhattacharjee, N. Gupta, hep-ph/0501191.
- [19] S. Hummer, M. Maltoni, W. Winter, C. Yaguna, Astropart. Phys. **34** (2010) 205-224; P. Mehta, W. Winter, JCAP **1103** (2011) 041.

- [20] Z. -z. Xing, S. Zhou, arXiv:1105.4114 [hep-ph].
- [21] E. Waxman, J. N. Bahcall, Phys. Rev. **D59** (1999) 023002.
- [22] R. Abbasi *et al.* [IceCube Collaboration], Phys. Rev. **D83** (2011) 092003; arXiv:1104.5187.
- [23] R. Gandhi, C. Quigg, M. H. Reno and I. Sarcevic, Astropart. Phys. **5** (1996) 81; Phys. Rev. D **58** (1998) 093009.
- [24] J. G. Learned, S. Pakvasa, Astropart. Phys. **3** (1995) 267-274.
- [25] A. Bhattacharya, R. Gandhi, W. Rodejohann, A. Watanabe, in preparation.
- [26] G. J. Feldman, R. D. Cousins, Phys. Rev. **D57** (1998) 3873-3889.